Light Metals 2014
Edited by: John Grandfield
TMS (The Minerals, Metals & Materials Society), 2014

WETTING CHARACTERISTICS OF CRYOLITE-BASED MELTS ON SPINELS SUBSTRATE

Reiza Z. Mukhlis[1], Muhammad Akbar Rhamdhani[1], Geoffrey Brooks[1], Kathie McGregor[2]
[1]Swinburne University of Technology, PO Box 218, Hawthorn, Victoria 3122, Australia
[2]CSIRO PSE, Box 312, Clayton South, Victoria 3169, Australia

Keywords: Sidewalls, Spinel, Wetting, Infiltration.

Abstract

Spinels have recently been proposed as ledge free sidewall material for aluminium smelter, mainly due to its low solubility in cryolite. A ledge-free sidewall will have a direct contact with electrolyte and therefore its wetting properties become important as it determine the penetration of the electrolyte into the sidewall which in turn may affect its corrosion level. In the present study, the wetting properties of cryolite based melts on various spinels substrates have been studied by sessile drop approach. The apparent contact angle of the melts on $NiFe_2O_4$ and $MgAl_2O_4$ substrates under argon atmosphere at 1030 °C was measured. It was found that spinels were wetted by the melts with apparent contact angles ranging from 9° to 19°. It was also observed that the capillary effect play a significant role in the infiltration of the melts into the substrates. The average infiltration rate was found to be 8.5 mm^3/s.

Introduction

Historically, conventional sidewalls for Hall-Heroult cell have been made from ramming paste and/or prebaked carbon blocks manufactured from the same materials as the carbon cathode blocks [1]. Due to lower electrical conductivity and higher resistance toward electrochemical wear, SiC and Si_3N_4-bonded SiC refractories, has been increasingly used as sidewall replacing traditional carbon based materials for over the last three decades [2]. The performance of both carbon and silicon carbide sidewalls are highly relied on the existence of a protective frozen electrolyte layer that contributed to the high energy inefficiency of the smelting process [3].

A ledge free sidewall offer solution to reduce energy losses through sidewall [4-7]. Moreover, with the application of ledge-free sidewalls, there is more volume available for anode and electrolyte bath, allowing higher cell capacity and productivity, and more predictable and controllable current efficiency [4]. A ledge-free sidewall will also be required if the emerging technology of inert anodes and wettable cathodes are to be implemented, as these application would lead to the alteration of the heat balance within the cell, with the amount of heat dissipated through the sidewalls likely to be lowered [5-7].

The environment within the Hall-Heroult cell is very extreme that require highly demanding properties of the ledge-free sidewall materials. The requisite properties of such sidewall are very much similar to the required properties of inert anodes materials [7-10]. Consequently, materials candidates for inert anodes would also be good candidates for ledge-free sidewall [7]. Recently, aluminate spinels and ferrite spinels has been proposed and assessed as ledge-free sidewalls [7, 11-14]. As refractories in general, spinels contain pores. The typical porosity level of sidewall materials is no higher than 25% [8].

Wetting characteristic of electrolyte bath and molten aluminium toward sidewall materials become important when the porous sidewall have a direct contact with the melts. The aluminium melts and electrolyte bath may penetrate into the sidewall through its pore and affect its corrosion [15].

To the authors' knowledge, there is no available data in the literature on the wetting of cryolite-alumina melts on Si_3N_4-bonded SiC refractories. However, there are numerous data available for NaF-AlF_3-alumina melts-carbon substrate system [16-19]. All of experiments conducted under inert atmospheres. It is understandable since carbon is easily oxidized under air atmosphere at the melting temperature of NaF-AlF_3-alumina mixture. Moreover, the use of inert atmosphere is important to avoid the formation of highly toxic hydrogen fluoride gas.

Since the experimental parameters i.e. experimental temperature and carbon quality were different, the values of the measured contact angle cannot be directly compared [16-19]. However, the general trend showed that carbon substrate is not wetted by the melts, with the contact angle ranging between 100° to 145°, and amorphous carbon wetted better than graphite. The increase of alumina content in the melts was found to increase wettability.

It should be noted however, that the above contact angle may not represent the true wetting characteristic of the NaF-AlF_3-alumina melts-carbon system in the real electrolysis cell. Complex gas composition in the cell determines the surface tension of the solid-gas and liquid-gas interface which in turn affect its wetting properties. The wetting of the electrolyte on carbonaceous material is also significantly affected by the electrode potential and its current density [3, 20]. When the carbon was cathodised, the angle of wetting decreased from 110° to about 30° as the current density increased to 4 A/cm^2 [20]. It is also worth to be noted that the presence of metallic aluminium in the electrolyte melts will increase wettability of the carbon materials [20, 21].

In the present paper, the wettability of nickel ferrite spinel and magnesium aluminate spinel substrates by cryolite-based melts was studied using the sessile drop method. The penetration of the melts into the spinels was also assessed in this study. An argon atmosphere was chosen in order to make the results comparable with the data available for NaF-AlF_3-alumina melts-carbon system.

Porosity, Melts Penetration and Contact Angle

Fully dense-non porous refractories might be impractical and uneconomical to be applied as sidewall in industrial scale Hall-Heroult cell. Indeed, pores can even somehow beneficial since it can act as a crack propagation stopper and enhance fracture toughness of the refractories. As a crack meet a pore in a porous ceramic, the crack tip becomes blunt that decreases the stress concentration at the crack tip which in turn increases the external

load needed to further propagate the crack [22]. However, pores on sidewall will promote the attack of electrolytes to the sidewalls when the sidewall materials wetted by the electrolytes.

Wettability of a refractory by electrolyte melts can be described by the contact angle (θ) at the line of contact of solid, liquid and gas phase and the work of adhesion. The contact angle is related to the three surface tensions of the interfaces solid-gas (γ_{SG}), solid-liquid (γ_{SL}) and liquid –gas (γ_{LG}), as defined by Young equation:

$$\cos\theta = \frac{\gamma_{SG} - \gamma_{SL}}{\gamma_{LV}} \qquad (1)$$

On the porous substrate, the melts tends to stay on the top of the substrate when the substrate is not wetted by the melts i.e. the contact angle is higher than 90°. The relevant equation to describe this phenomenon is the Laplace equation:

$$\Delta P = \frac{2\gamma_{LV}\cos\theta}{r} \qquad (2)$$

where ΔP is the capillary pressure i.e. the pressure required to force or restrain entry of liquid, and r is the capillary radius. When the substrate is wetted by the melts, i.e. contact angle is lower than 90° (hence ΔP value is negative), the melts will readily penetrate into the pore.

If the open pores on the surface of the substrate are treated as capillaries, the volumetric penetration rate (dV/dt) of the melts into the pore can be expressed by Hagen-Poiseuille's law:

$$\frac{dV}{dt} = \frac{\pi r^4 \Delta P}{8\eta h} \qquad (3)$$

where dV is the volume change ($=\pi r^2 dh$), h is the height of liquid front or depth of penetration, t is the time, and η is the dynamic viscosity of the liquid. By substituting ΔP from equation (1) to equation (2) results in Washburn's equation as:

$$\frac{dh}{dt} = \frac{r\gamma_{LV}\cos\theta}{4\eta h} \qquad (4)$$

Materials and Method

Substrate Preparation

Nickel ferrite ($NiFe_2O_4$) and magnesium aluminate ($MgAl_2O_4$) spinels substrates were prepared from pre-synthetized spinel powders that were made through solid state sintering of its oxide precursors as detailed in [12]. About 8 grams of powders were pressed uniaxially into green discs in a 25 mm diameter die at a compaction pressure of 125 MPa. The green discs were subsequently sintered in a muffle furnace under air atmosphere at 1200 to 1600 °C for 24 to 55 hours to obtain substrates with several different porosity levels. The sintered discs were then ground and polished by diamond paste down to 1 µm.

Porosity and Surface Roughness Measurement

The porosity of the substrate was determined by the ASTM method C20-00. The apparent porosity of the substrates was found to be in the range of 2 to 13%, which is in the acceptable porosity range for sidewall applications. The bulk density and apparent porosity of each batch of samples are detailed in Table 1.

Table I. Bulk Density and Apparent Porosity

Material	Sintering		Bulk Density (g/cm^3)	Apparent Porosity (%)	R_A
	Temp. (°C)	Time (h)			
$MgAl_2O_4$	1550	30	3.01 ± 0.02	13.4 ± 0.2	0.45 ± 0.02
	1600	24	3.1 ± 0.02	8.6 ± 0.4	0.47 ± 0.03
	1600	30	3.2 ± 0.01	6.3 ± 0.2	0.29 ± 0.03
$NiFe_2O_4$	1200	24	4.1 ± 0.04	23 ± 0.8	0.59 ± 0.04
	1300	24	4.7 ± 0.02	10.6 ± 0.4	0.33 ± 0.02
	1600	24	5.15	2.1	0.27 ± 0.04

The substrate surface roughness was measured by a Talysurf profilometer. The typical surface profile of the substrate is shown in Figure 1. It was found that the roughness parameter R_A value were in the range of 0.27 to 0.59 µm. The relatively high value of R_A is due to the porosity of the substrate that is represented by negative amplitude in Figure 1. In general, samples with higher porosity level have higher R_A value (see Table 1).

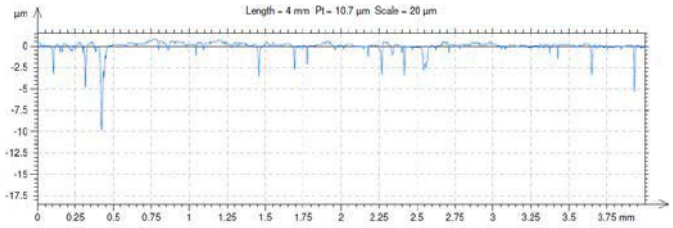

Figure 1. Surface profile measurement result for $NiFe_2O_4$ substrate with 2 % porosity.

Electrolyte Droplet Preparation

As purchased synthetic cryolite powder containing at least 97% Na_3AlF_6 were mixed with AlF_3 (analytical reagent) and various amount of Al_2O_3 (99.7% purity) to obtain cryolite-based electrolyte with cryolite ratio of 2.3. Three different alumina content of: 0 wt%, 6 wt% and 11 wt% were used in the study.

The desired amounts of cryolite, AlF_3 and alumina powders were first weighed and well mixed in a plastic container. The powders were previously placed in a vacuum oven heated to 125 °C to remove the traces of moisture. To ensure homogeneity, the mixture was then melted in a furnace at 1030 °C under argon atmosphere for 2 hours. The solidified bath was subsequently crushed into small pieces of around 0.1 g to be used as specimen for wetting experiments.

Wetting Experiments

The wetting experiments were conducted in a gas-tight horizontal tube furnace. A schematic diagram of the furnace arrangement is shown in Figure 2.

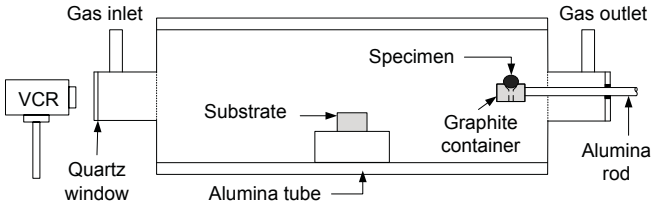

Figure 2. Schematic diagram of the experimental setup used for measuring contact angle using the sessile drop approach.

The substrate was adhered to an alumina holder by high purity alumina paste. The paste was also used to adjust the levelness of the substrate. The levelness was checked with spirit level and laser leveler. The specimen, i.e. small piece of solid cryolite-based electrolyte with various alumina additions, was placed in a hollow graphite container that was fitted to an alumina rod.

The wettability experiments were performed at 1030 °C under high purity argon atmosphere. To achieve the inertness of the atmosphere, the furnace was placed under vacuum prior to the experiment and high purity argon gas was flown into the furnace through gas drying system containing drierite for at least 30 minutes with a flow rate of 1 l/min. The argon was then continuously flown during the experiment at a rate of 0.3 l/min. With a heating rate of 200 °C/h, the furnace was flushed with argon for at least 5 hours before it reached the experimental temperature.

At the beginning of the experiment, the graphite container was placed in the cold zone of the furnace while the substrate was placed at the centre of the furnace as illustrated in Figure 2. The arrangement remain unchanged for 30 minutes after the furnace reach the set temperature to make sure the temperature of the substrate was in a steady state condition.

The alumina rod that was assembled to the graphite container and specimen was then slowly and carefully pushed toward the hot zone of the furnace. To avoid thermal shock, a pace of 1 cm/min was used when pushed the rod. Once the specimen fully melted, it will drop on the substrate as it did not wetted the graphite container. The alumina rod was then pulled out of the hot zone step by step at a pace of 5 cm per 10 minutes until it reached the cold zone. After holding the experimental temperature for 1 h, the furnace was allowed to cool.

All process starting from the introduction of the specimen to the hot zone was captured by a video camera through a quartz window located on the front of the horizontal alumina tube. The camera was placed on a tripod that was well aligned with the position of the substrate and specimen. A laser leveler was used prior to each experiment to ensure the alignment. The focus and the zoom of the camera were set prior to the experiment. Digital still images from the recorded film were used to determine the contact angle of the droplet by ImageJ software. The contact angle calculation in this approach is based on the fitting of the Young-Laplace equation to the image data [23].

Results and Discussion

Preliminary Experiments

Initially, the wetting experiments were conducted following method used by Meunier [19] which was slightly different with the method detailed above. The only significant difference was that instead of placing the electrolyte pellet in graphite container, the pellet was directly placed on the top of the substrate at the cold zone which then pushed forward to the hot zone when the experimental temperature was reached.

It was found that electrolyte pellet gradually vanished before it melted completely to form an angle with the substrate. The pellet started to melt after held in the hot zone for about 3 minutes and disappeared in just 2 minutes after that (see Figure 3).

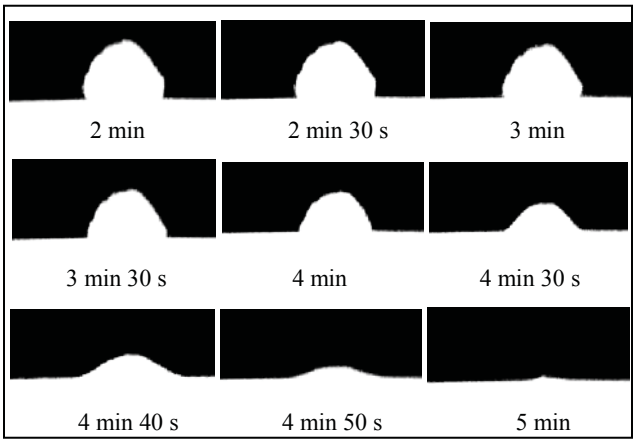

Figure 3. Gradual change of the shape of electrolyte pellet/melt for the duration of 2 min to 5 min after placed in the hot zone.

There were two possible explanations for the pellet to be disappeared before it completely melt and forms any angle with the substrate. It was either due to evaporation of the melts or due to penetration of the melts into the substrate through its pores. At very high evaporation rate, once parts of the pellet melted, it will immediately evaporate. This condition makes the measurement of contact angle impossible.

In order to examine whether the melts was immediately vanished due to high evaporation rate, several experiments were conducted at various temperature and various argon flow rate, both were lower than that was described in the experimental method section of this paper. It was expected that by lowering the experimental temperature and argon flow rate, the evaporation rate could be minimized. However, no significant differences were noticed. The pellets still disappeared gradually before it forms any meaningful contact angle.

Experiments on graphite substrate that have same porosity level as the spinels substrates were then conducted. The angle of contact between the electrolyte melts and the graphite substrate can easily be measured as the melts stayed on the substrate during the duration of the experiments. It was found that the contact angle was in the range of 110 to 130°. The melts did not disappear even for extended experiments duration up to 3 h. In the case of 10 minutes experiments, there are no significant changes in the

weight of the electrolyte before and after experiments. This indicated that the evaporation rate was very low. This also indicated that cryolite did not penetrate into graphite substrate within 10 minutes duration of experiment. The latter hypotheses was supported by further EDX analysis that shown no evidence of sodium, fluorine and aluminium elements at the interior of the substrate.

There were no meaningful data regarding contact angle and penetration rate can be obtained from several experiments conducted with the above setup. However, these experiments provide valuable information which confirms that the electrolyte melts infiltrated into the substrate and that the evaporation rate of the electrolyte at the defined experimental conditions was very low hence negligible.

Wetting of Electrolyte on Spinel Substrate

Wettability of the cryolite-based electrolyte on nickel ferrite and magnesium aluminate substrate was studied by mean of apparent contact angle measurements. The apparent contact angle in this context was defined as the angle between the melts to the substrate taken at 1s after the melts drop onto the substrate.

The term of apparent contact angle was used instead of contact angle as the equilibrium condition may have not been achieved. Equilibrium took place when there are no chemical reactions between all the phases involved i.e. solid, liquid and gas; and there are no mass transfer between the phases. It is true that there was no mass transfer to the gas phase as the evaporation rate is negligible. Noting that the contact angle was taken at 1 s after contact, the chemical reaction and mass transfer from solid to liquid may also be neglected even though there are limited solubility of spinels in cryolite [11, 12]. However, there was mass transfer from liquid to solid as the melts indeed infiltrate through the pores and the steady state condition has not been achieved.

Figure 4 shows the images captured for various alumina contents of the melts on $MgAl_2O_4$ substrates with 13% porosity. The associated measured contact angles versus alumina content are plotted in Figure 5.

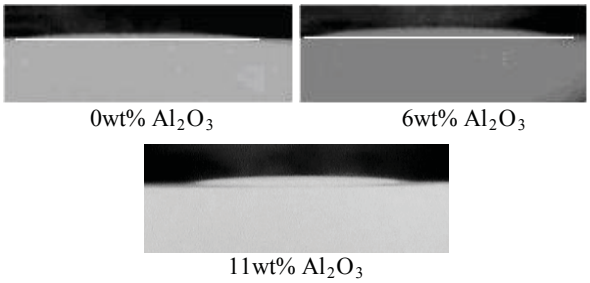

Figure 4. Image of electrolyte droplet on $MgAl_2O_4$ substrate captured at 1 s after the melts dropped. White line at 0wt% and 6wt% Al_2O_3 was drawn to distinguish the melts and the substrate.

The wettability of the electrolyte on $MgAl_2O_4$ substrate was found to decrease as the alumina content in the electrolyte increased. The measured apparent contact angle value was 19.4°, 12.2°, and 9.3° for electrolyte contains 0 wt%, 6wt%, and 11wt% alumina, respectively.

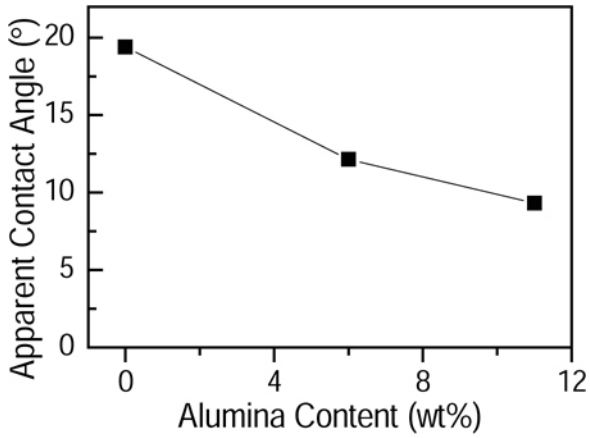

Figure 5. Measured contact angles of electrolyte with different alumina content on $MgAl_2O_4$ substrates contain 13% porosity.

The above trend can be explained by considering the surface tension of the melts. As described in Equation (1), contact angle is determined by the surface tensions. When the value of γ_{SG} - γ_{SL} is constant, the increase in γ_{LV} increases the contact angle. In Na_3AlF_6 –AlF_3 –Al_2O_3 systems at 2.35 cryolite ratio, the surface tension of the melts increase as more alumina is added to the mixture [24].

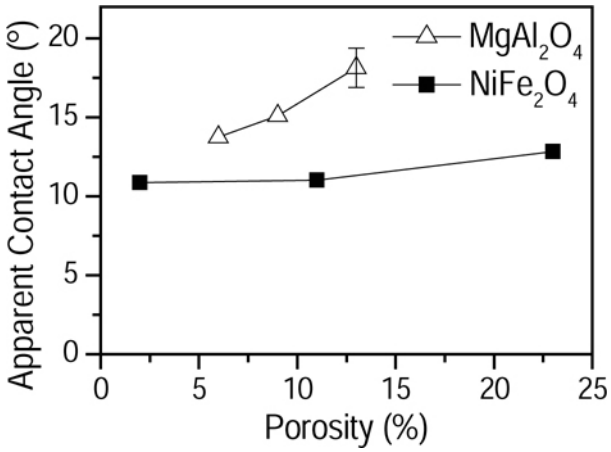

Figure 6. Measured apparent contact angles of pure electrolyte (0wt% Al_2O_3) on different porosity content of substrates.

Figure 6 presents the trend in the measured contact angles of pure electrolyte for different porosity level of $MgAl_2O_4$ and $NiFe_2O_4$ substrates. In general, the figure shows that the apparent contact angle was increased as the porosity increases. The figure also shows that $NiFe_2O_4$ wetted better than $MgAl_2O_4$ and the effect of porosity was more pronounced in $MgAl_2O_4$. Sample with high porosity content have rougher surface, represented by higher R_A value (Table 1). Surface roughness is one of the factors that may inhibit the spreading of the liquid, which in turn resulting in high contact angle. The roughness however, may be spontaneously invaded depending on the surface pattern and the wetting properties of the liquid [25]. Further investigation on the porosity shape and size would be required to further explain the trend.

Infiltration Rate of Electrolyte

As it was impossible to detect the liquid front and hence the depth of melts infiltration over time, the infiltration rate of the electrolyte to the substrate was measured based on the change of volume of the droplet stayed on the top of the substrate over time. The droplet was assumed to be in the spherical cap shape, which the volume is:

$$V = \frac{\pi h}{6}\left(3a^2 + h\right) \qquad (5)$$

where a is the radius of the base of the cap, and h is the height of the cap. The change of the volume of the droplet stayed on the top of the substrate is the inverse of the volume change of the melts infiltrate to the substrate. The volumetric infiltration rate was then defined as volume of the droplet on the top of the substrate over the time needed for the droplet to disappear.

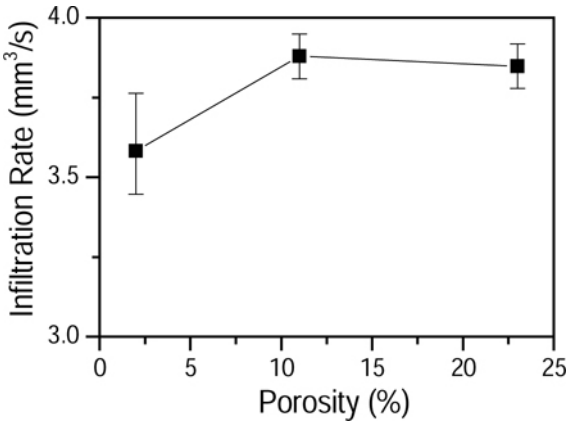

Figure 7. Infiltration rate of pure electrolyte melts on $NiFe_2O_4$ substrates.

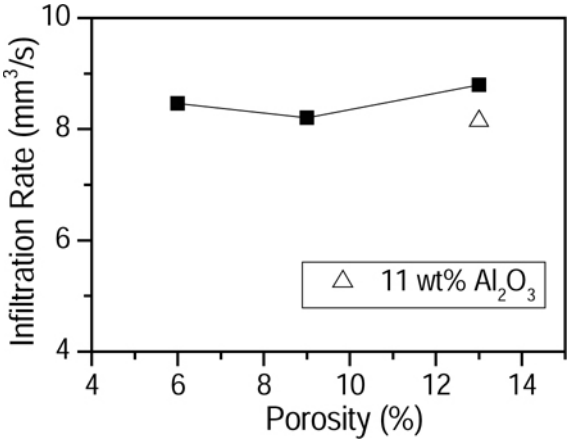

Figure 8. Infiltration rate of pure electrolyte melts on $MgAl_2O_4$ substrates.

Figures 7 and 8 show the infiltration rate of electrolyte melts on $NiFe_2O_4$ and $MgAl_2O_4$ substrates, respectively. In general, the electrolyte melts infiltrate to the substrate for less than 10 seconds. There was no clear correlation between the porosity levels with the infiltration rate can be deducted from the results of current study. The amount of melt available for infiltration was too small. Moreover, the melt infiltration is also affected by the size and shape of the porosity as well as its distribution throughout the substrate surface.

It is interesting to note that the infiltration rate of electrolyte melts on $MgAl_2O_4$ was higher than that of $NiFe_2O_4$ even though $NiFe_2O_4$ had better wettability. According to Equation (4), the infiltration rate of the melts to the substrate should be low if the contact angle is high. One possible explanation to this contradicting phenomenon was that on $MgAl_2O_4$, due to high infiltration rate, the melts penetrated before it spread further, which in turn resulted in the high apparent contact angle

The infiltration volume rate on $MgAl_2O_4$ was found to be lower for electrolyte melts with high alumina content. It was in agreement with Equation (4) as the viscosity of the melts was higher at high alumina concentration. Recalling results presented in Figure 5, the apparent contact angle was also lower at high alumina concentration. However, the value of 8.15 mm^3/s of the infiltration rate was within measurement error. An infiltration rate measurements method developed by Grundke et al. [26] that was based on mass change may provide more accurate results. However, the nature that cryolite penetration measurement has to be conducted in a relatively high temperature and controlled atmosphere, make such method be very difficult to be applied.

Scanning electron microscopy (SEM) and energy dispersive x-ray spectroscopy (EDX) analysis on the tested substrate has been performed to check the depth of infiltration of the melts. Figure 9 shows the element mapping of the cross sectioned $MgAl_2O_4$ substrate that after wetted by pure electrolyte (0wt% alumina). Light area indicates high element concentration.

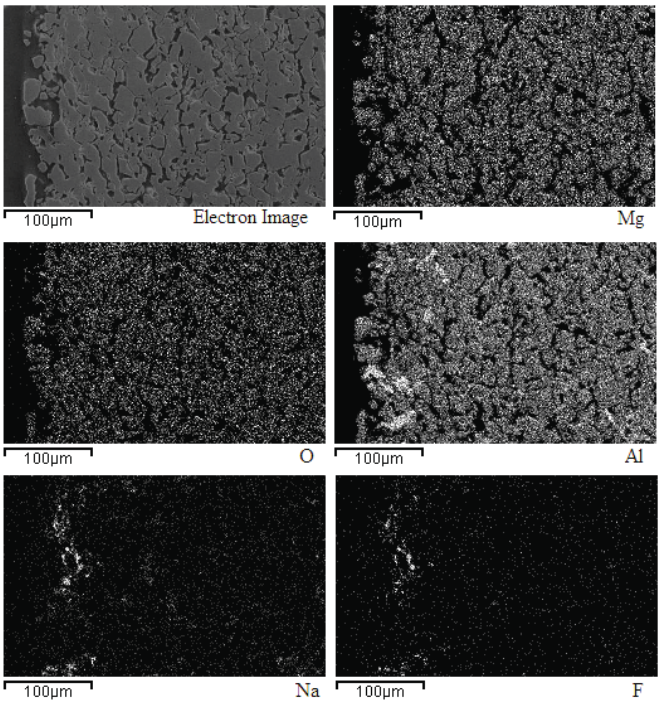

Figure 9. Elemental mapping of cross sectioned $MgAl_2O_4$ substrate after wetted by pure electrolyte (0 wt% Al_2O_3).

The EDS analysis showed that the traces of sodium and fluoride was found at the substrate up to 300 µm depth with the higher concentration of the elements in the pore, particularly up to 20 µm depth. This clearly indicated that the electrolyte melts infiltrate the substrate through its pore. Some traces of sodium and fluoride were also found inside the grain. It was true that the contact angle measurements were conducted for 1 s and the infiltration rate measurements were conducted for 10 s only. However, the substrate and the droplet stayed in the hot zone at temperature for 1 hour and were not removed from its position until the furnace cooled down naturally. This condition may enable the sodium and fluoride to diffuse into the grain.

Conclusions

Cryolite-based electrolyte melts was found to have a good wettability with $MgAl_2O_4$ (and $NiFe_2O_4$) spinels. The apparent contact angle was in the range of 9° to 19° with the higher contact angle for the melts with high alumina content. Good wettability make the melts readily infiltrate through the pore of any porous substrate. If the spinels are intended to be applied as sidewall materials for aluminium smelter, such surface modification will be required since the penetrated melts influenced its corrosion.

References

1. M. Sorlie and H.A. Oye, (1989) "Evaluation of Cathode Material Properties Relevant to The Life of Hall-Heroult Cells", *Journal of Applied Electrochemistry,* (19) (1989) 580-58.
2. G. Brooks et al., "Challenges in Light Metals Production", *Mineral Processing & Extractive Metallurgy: Transactions of the Institution of Mining & Metallurgy, Section C*, (116) (2007) 25-33.
3. K. Grjotheim and B.J. Welch, *Aluminium Smelter Technology,* 2nd ed., (Düsseldorf: Aluminium-Verlag, 1988), 146-152, 181-190.
4. D.D. Juric, et al., "Ledge Free Aluminium Smelting Cell", *US Patent*, (1997), No. 5667664.
5. W.T. Choate and J.A.S. Green, "U.S. Energy Requirements for Aluminum Production: Historical Perspective, Theoretical Limits and New Opportunities", *prepared under Contract to BCS, Incorporated, Columbia, MD., U.S. Dept. Energy, Energy Efficiency and Renewable Energy*, Washington, D.C., 2003.
6. H. Kvande, and W. Haupin, Inert anodes for Al smelters: Energy Balances and Environmental Impact. *JOM*, 53 (5) (2001), 29-33.
7. R. Mukhlis, M.A. Rhamdhani, and G. Brooks, "Sidewall Materials for Hall-Heroult Process", *Light Metals 2010*, ed. J.A. Johnson, (Warrendale, PA:TMS, 2010), 883-888.
8. B.J. Welch and A.E. May, "Materials Problem in Hall-Heroult Cells", *8th Int. Leichmetalltag.*, Leoben-Vienna, (1987), 120-125.
9. R.P. Pawlek, "Methods to Test Refractories Against Bath Attack in Aluminum Electrolysis Pots", *Aluminium*, 70 (1994), 555-559.
10. I. Galasiu, R. Galasiu & J. Thonstad, (2007), *Inert Anodes for Alurninium Electrolysis,* (Düsseldorf: Aluminium-Verlag, 2007).
11. X.Y. Yan, M.I. Pownceby, and G. Brooks, "Corrosion Behavior of Nickel Ferrite-Based Ceramics for Aluminum Electrolysis Cells, *Light Metals 2007*, ed. M. Sorlie, (Warrendale, PA:TMS, 2007) 909-913.
12. X.Y. Yan, R.Z. Mukhlis, M.A. Rhamdhani and G.A. Brooks, (2011), "Aluminate Spinels as Sidewall Lining for Aluminium Smelters", *Light Metals 2011*, ed. S.J. Lindsay, (Warrendale, PA: TMS, 2011), 1085–1090.
13. R.Z. Mukhlis et al., "Fabrication of Spinel Composites for Sidewall of Al Smelter Application", *Proceedings of European Metallurgical Conference –Volume 3*, (Dusseldorf: GDMB, 2011) 865–880.
14. S.A. Nightingale, R.J. Longbottom, and B.J. Monaghan, "Corrosion of Nickel Ferrite Refractory by Na_3AlF_6–AlF_3–CaF_2–Al_2O_3 Bath. *Journal of the European Ceramic Society*, (33) (13-14) (2013), 2761–2765.
15. D. Harris and G. Oprea, "Cryolite Penetration Studies on Barrier Refractories for Aluminium Electrolytic Cells*", Light Metals 2000*, ed. R. D. Peterson, (Warrendale, PA:TMS, 2000), 419-427.
16. K. Matiasovsky, M. Paucirova, and M. Malinovsky, *Chemicke Zvesti*, (17) (1963) 181
17. E.A. Zhemchuzhina, Dissertation, Moscow Institute of Steel and Alloys, Moscow, 1962
18. J.B. Metson et al., "The Anode Effect Revisited", *Light Metals 2002*, ed. W. Schneider, (Warrendale, PA:TMS, 2002), 239-244.
19. P. Meunier et al., "Effect of Dopants on Wetting Properties and Electrochemical Behaviour of Graphite Anodes in Molten Al_2O_3 – Cryolite Melts", *Journal of Applied Electrochemistry*, (39) (6) (2009), 837-847.
20. Z.X. Qui, Q.B. Wei, and K.T. You, "Studies on Wettability of Carbon Electrodes in Aluminium Electrolysis", *Aluminium*, (59) (1983) 670-673.
21. P. Fellner and Z. Lubyova, "Equilibrium Between Aluminium and The Cryolite Melt Containing Lithium Fluoride", *Chemical Papers* (40) (2) (1986) 145-151.
22. Z.Y. Deng, et al., "Effect of Agglomeration on Mechanical Properties of Porous Zirconia Fabricated by Partial Sintering", *Journal of American Ceramic Society* (85) (2002), 1961-1965.
23. A.F. Stalder, T. Melchior, M. Müller, D. Sage, T. Blu, M. Unser, "Low-Bond Axisymmetric Drop Shape Analysis for Surface Tension and Contact Angle Measurements of Sessile Drops," *Colloids and Surfaces A: Physicochemical and Engineering Aspects*, (364) (1-3) (2010), 72-81.
24. R. Fernandez and T. Ostvold, "Surface tension and density of molten fluorides and fluoride mixtures containing cryolite", *Acta Chemica Scandinavica*, (43) (1989), 151-159.
25. J. Bico, C. Tordeux, and D. Quere, Rough Wetting, Europhysic Letters, (55) (2) (2001), 214-220.
26. K. Grundke et al., "Wetting measurements on smooth, rough and porous solid surface", *Progress in Colloid and Polymer Science*, (101) (1996), 56-68.